Available online at www.sciencedirect.com
SCIENCE DIRECT®
Surface Science 553 (2004) 39–49
SURFACE SCIENCE
www.elsevier.com/locate/susc

Probing the chemistry of CH_3I on Pt–Sn alloys

Chameli Panja, E.C. Samano [1], Najat A. Saliba, Bruce E. Koel *

Department of Chemistry, University of Southern California, Los Angeles, CA 90089-0482, USA

Received 20 February 2003; accepted for publication 13 November 2003

Abstract

Adsorption and reaction of CH_3I (methyl iodide) on Pt(1 1 1) and the (2×2) and ($\sqrt{3} \times \sqrt{3}$)R30° Sn/Pt(1 1 1) surface alloys was investigated primarily by using temperature programmed desorption (TPD) and high-resolution electron energy loss spectroscopy (HREELS). CH_3I adsorbs molecularly on Pt(1 1 1) at 100 K, and 34% of the adsorbed CH_3I monolayer decomposes during heating above 200 K in TPD. Competition occurs during heating within the chemisorbed layer between hydrogenation to produce methane and dehydrogenation that ultimately leads to adsorbed carbon. Alloying Sn into the Pt(1 1 1) surface decreases the heat of adsorption and the amount of decomposition of CH_3I. Alloyed Sn slightly reduces the CH_3I adsorption bond energy from 13.4 kcal/mol on Pt(1 1 1) to 11.4 kcal/mol on the (2×2) alloy with $\theta_{Sn} = 0.25$ and 9.3 kcal/mol on the ($\sqrt{3} \times \sqrt{3}$)R30° Sn/Pt(1 1 1) alloy with $\theta_{Sn} = 0.33$. More notably, the Sn–Pt alloy surface strongly suppressed CH_3I decomposition. Only 4% of the adsorbed CH_3I monolayer decomposed on the (2×2) Sn/Pt(1 1 1) surface, and no decomposition of CH_3I occurred on the ($\sqrt{3} \times \sqrt{3}$)R30° Sn/Pt(1 1 1) surface during TPD. Methane was the only hydrocarbon desorption product observed during TPD. These results point to the importance of adjacent "pure Pt" threefold hollow sites as reactive sites for CH_3I decomposition. Finally, we note that CH_3I, and presumably the other short-chain alkyl halides, are not reactive enough on Pt–Sn alloys to serve as convenient thermal precursors for preparing species small alkyl groups such as CH_3(a) for important basic studies of the reactivity and chemistry of alkyl groups on Pt–Sn alloys. Another approach is required such as the use of a CH_3-radical source or non-thermal activation of adsorbed precursors via photodissociation or electron-induced dissociation (EID).

Keywords: Alloys; Platinum; Tin; Halides; Thermal desorption; Electron energy loss spectroscopy (EELS); Chemisorption; Surface chemical reaction

1. Introduction

Generation of alkyl groups and studies of their reactivity on metal surfaces has been of interest for many years [1–11]. An understanding of this chemistry is important because of the role of these species as reaction intermediates in heterogeneous catalysis over metals [12,13].

The smallest alkyl group is methyl (CH_3) and a variety of techniques have been developed to prepare surface-bound methyl species on metal single crystals in UHV environments, including thermal activation of methane from molecular beams [14], CH_3^+ ion beams [15], and thermal pyrolysis sources

* Corresponding author. Tel.: +1-213-7404126; fax: +1-213-7403972.
E-mail address: koel@chem1.usc.edu (B.E. Koel).
[1] Permanent address: Centro de Ciencias de la Materia Condensada-UNAM, Ensenada, BC, México.

0039-6028/$ - see front matter © 2003 Published by Elsevier B.V.
doi:10.1016/j.susc.2003.11.038

using azomethane as a precursor [16–18]. The most frequently used method involves the use of alkyl halides as precursors which can be thermally or photochemically activated on the surface to cleave the carbon-halogen bond [1–11]. For example, Zaera and co-workers have shown that adsorbed methyl groups can be prepared in this manner from CH_3I on Pt(1 1 1) above 200 K [4,5]. Subsequent thermal chemistry of the methyl groups involves a competition between hydrogenation and dehydrogenation resulting in desorbed methane and chemisorbed methylene, respectively, depending on the initial coverage on Pt(1 1 1) [4,5,19]. No C–C bond coupling of the adsorbed methyl groups on Pt(1 1 1) was observed [19].

Recently, we have shown that alloying Sn into a Pt(1 1 1) surface strongly affects the decomposition of several saturated and unsaturated hydrocarbons [20–25]. To extend these studies to include probing the chemistry of chemisorbed CH_3 groups, we report the investigation of methyl iodide adsorption and decomposition on two Sn/Pt(1 1 1) surface alloys. The (2×2) Sn/Pt(1 1 1) alloy thermally dissociates CH_3I to a small extent, helping to elucidate $CH_{3(a)}$ and $CH_{2(a)}$ reactions on this surface. However, CH_3I was reversibly adsorbed on the $(\sqrt{3}\times\sqrt{3})$R30° Sn/Pt(1 1 1) alloy with no decomposition during heating in TPD, so this approach is not reliable for probing the chemistry of $CH_{3(a)}$ and other alkyl group on Pt–Sn alloys. HREELS was used, however, to identify the existence of adsorbed CH_3 groups on the (2×2) Sn/Pt(1 1 1) surface alloy.

2. Experimental methods

All experiments were performed in a two-level stainless steel UHV chamber with a base pressure of 8×10^{-11} Torr as described elsewhere [26]. It was equipped with a four-grid, low energy electron diffraction (LEED) optics, double-pass cylindrical mirror analyzer (CMA) for Auger electron spectroscopy (AES), ion sputtering gun, UTI-100C quadrupole mass spectrometer (QMS) for temperature programmed desorption (TPD), HREELS spectrometer, and various metal and gas dosing facilities. The HREELS results shown herein were obtained later in a three-level UHV chamber with a base pressure of 2×10^{-10} Torr, as has been previously described [24]. The bottom level of this chamber contained an LK2000 spectrometer for HREELS.

The Pt(1 1 1) crystal was cleaned by repeated cycles of Ar^+-ion sputtering and O_2 exposures at $P_{O_2} = 5\times10^{-8}$ Torr with the crystal at 1100 K. The surface purity and long-range order were verified by AES and LEED, respectively. The crystal could be resistively heated to 1200 K and cooled to 90 K by using a liquid-nitrogen reservoir. The temperature was measured by a chromel–alumel thermocouple spot-welded directly to the crystal.

All TPD experiments were performed by heating at a constant rate of 4 K/s. The HREELS spectra were recorded in the specular scattering direction at an incident angle of 60° from the surface normal and incident electron beam energy of 1 eV. The overall energy resolution of the spectrometer was less than 6 meV (50 cm^{-1}) and the count rates at the elastic peak were 100 kHz for clean Pt(1 1 1). The spectra reported were normalized to the intensity of the elastic peak and taken with the sample held at a temperature of 100 K.

Methyl iodide (CH_3I) (Aldrich Chemical Company, 99.5% purity) was used as received. It was dosed onto the crystal through a Varian® leak valve connected to a multichannel-array gas doser positioned directly in front of the crystal surface. The dose measurements reported here were not corrected for ion gauge sensitivity or any enhancement by the multichannel array doser.

Following the work of Paffett and Windham [27], the (2×2) Sn/Pt(1 1 1) and the $(\sqrt{3}\times\sqrt{3})$R30° Sn/Pt(1 1 1) ordered surface alloys were prepared by evaporating Sn onto the clean Pt(1 1 1) surface at 300 K and subsequently annealing the sample to 1000 K for 10 s. Depending upon the initial Sn coverage, the annealed surface exhibited a (2×2) or $(\sqrt{3}\times\sqrt{3})$R30° LEED pattern. These patterns arise from "surface alloys" that are formed which contain no second-layer Sn atoms [28]. The (2×2) structure has $\theta_{Sn} = 0.25$ in the top layer and a 2D structure like the (1 1 1) face of the bulk Pt_3Sn crystal. The other is a substitutional alloy of composition Pt_2Sn with $\theta_{Sn} = 0.33$ [27,28]. These

surfaces are quite "flat", but there is an outward buckling of Sn above the Pt-surface plane of 0.20 Å [28]. The (2×2)-Sn/Pt(1 1 1) and the ($\sqrt{3}\times\sqrt{3}$)R30°-Sn/Pt(1 1 1) surface alloys will be referred to as the (2×2) and $\sqrt{3}$ alloys, respectively, for brevity in the rest of this paper.

3. Results and discussion

CH_3I adsorption was carried out on Pt(1 1 1) and both Sn/Pt(1 1 1) alloys at 100 K. The coverages used throughout this paper are referenced to the Pt(1 1 1) surface-atom density of 1.51×10^{15} atoms/cm^2 corresponding to $\theta = 1.0$ ML. Adsorption and desorption kinetics were probed by TPD and surface reactions were investigated using TPD and HREELS. We will discuss the TPD results first, and then consider the findings in the HREELS experiments.

The main desorption products during TPD from Pt(1 1 1) were H_2, CH_4 and CH_3I. Fig. 1 shows the CH_3I TPD curves following different CH_3I exposures on Pt(1 1 1) at 100 K. H_2 and CH_4 desorption will be considered later, as shown in Figs. 2 and 3. Iodine also desorbs from Pt(1 1 1) as atoms in the 500–800 K temperature range, as observed by Henderson et al. [1]. C_2H_x and higher order hydrocarbons were monitored during our TPD, but they were not detected. These results for Pt(1 1 1) are consistent with previous studies [1,4,5].

Low coverages of CH_3I on Pt(1 1 1) were irreversibly adsorbed; i.e., no molecular CH_3I desorption occurs in TPD after exposures of 0.08 L or less. CH_3I desorption occurs with a peak at 256 K after a 0.16 L dose. This high temperature peak shifts lower to 233 K and a new peak appears at 133 K at higher coverages. The intensity of the low temperature peak continues to increase with higher exposures, and we associate this peak with desorption of a condensed multilayer film of methyl iodide on Pt(1 1 1). This low temperature peak at 133 K also exists on both alloys for CH_3I multilayers.

On the (2×2) alloy, a CH_3I desorption peak occurs at 220 K due to partially reversible adsorption even following low exposures of CH_3I,

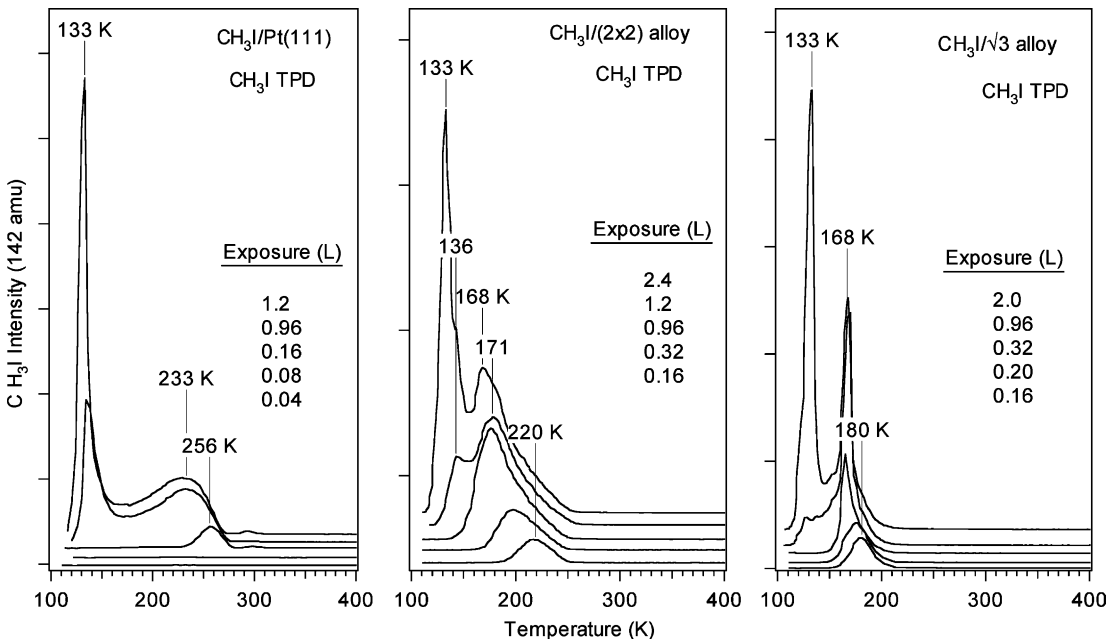

Fig. 1. Methyl iodide TPD traces following CH_3I exposures on Pt(1 1 1) and the (2×2) and $\sqrt{3}$ alloys at 100 K. The *y*-axis scales on these graphs are not the same, but have been rescaled for illustrative purposes.

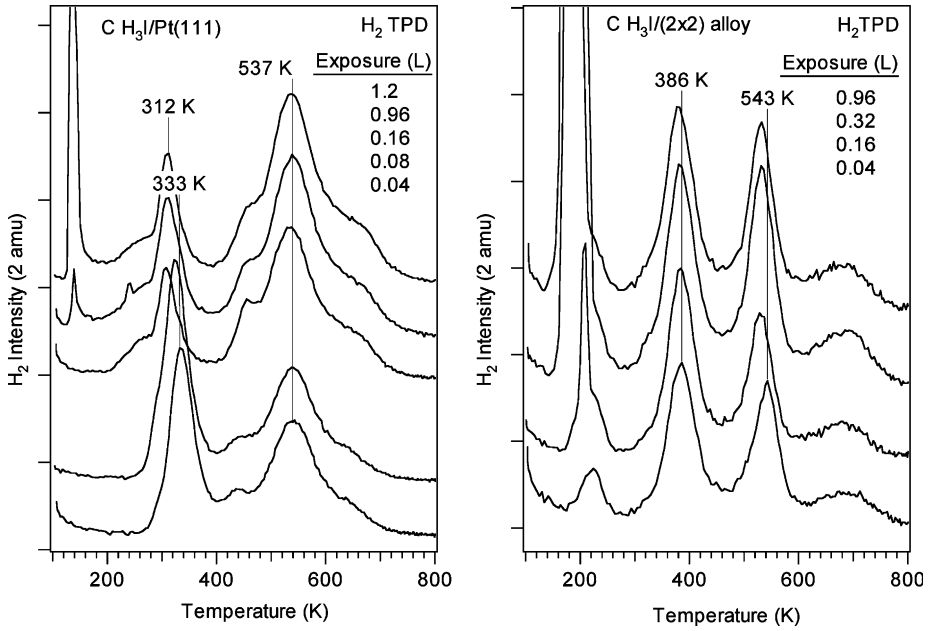

Fig. 2. H_2 TPD traces after a series of CH_3I exposures on Pt(1 1 1) and the (2×2) alloy at 100 K. The *y*-axis scales on these graphs are not the same, but have been rescaled for illustrative purposes.

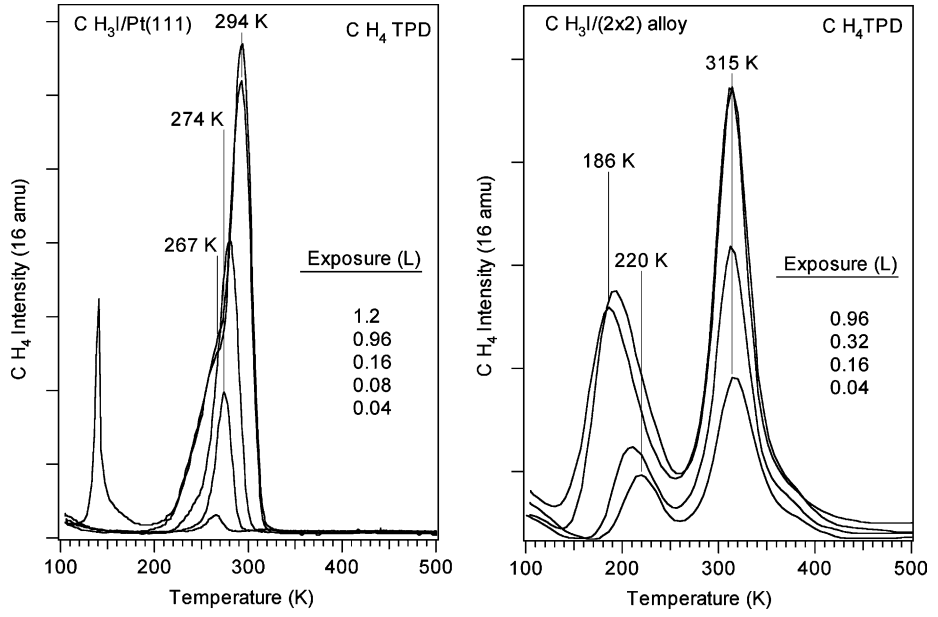

Fig. 3. CH_4 TPD curves following increasing CH_3I exposures on Pt(1 1 1) and the (2×2) alloy at 100 K. The *y*-axis scales on these graphs are not the same, but have been rescaled for illustrative purposes.

as shown in Fig. 1. This peak shifts to 171 K near saturation of the monolayer. In contrast to the behavior on Pt(1 1 1), evolution of molecular CH_3I occurs in TPD even after the lowest exposure of

0.04 L (not shown). On the $\sqrt{3}$ alloy, CH_3I desorbs in a single, relatively narrow peak at 180 K at low coverages in the monolayer. This peak shifts to 168 K at monolayer saturation. On this alloy, there was completely reversible adsorption of CH_3I at any coverage and no desorption of other species was detected.

Coverage-dependent shifts in the CH_3I desorption peak from the monolayers shown in Fig. 1 are often explained by repulsive lateral interactions between adsorbates which decreases the activation energy for desorption with increasing initial coverage. Support for this explanation here comes from the work of Zaera and Hoffman [5] in which they found that CH_3I chemisorbs on Pt(1 1 1) with the C–I bond tilted with respect to the surface at low coverages, but reoriented to position the C–I bond perpendicular to the surface as the adsorbate coverage is increased.

The chemisorption bond energy of CH_3I is reduced on both of the Sn–Pt alloys compared to that on clean Pt(1 1 1). This reduction can be directly observed with TPD, because the adsorption energy is equal to the desorption activation energy, assuming a negligible activation energy for molecular adsorption which should easily be satisfied for this weakly bonded system. The CH_3I desorption peak at low exposures shifts from 256 K on Pt(1 1 1) to 220 and 180 K on the (2×2) and $\sqrt{3}$ alloys, respectively. Thermal desorption activation energies, E_d, were estimated from the peak temperatures in the TPD curves that correspond to about 10% of the monolayer saturation coverage to minimize the influence of inter-molecular lateral interactions. By means of Redhead analysis [29], assuming first order desorption kinetics and a pre-exponential factor of 10^{11} s^{-1} [30], we estimate that E_d decreases from 13.4 kcal/mol on Pt(1 1 1) to 11.4 and 9.3 kcal/mol on the (2×2) and $\sqrt{3}$ alloys, respectively. These values can also be compared to our estimate of E_d for the sublimation energy of physisorbed CH_3I, condensed in the multilayer and desorbing near 133 K, of 8 kcal/mol assuming a pre-exponential factor of 10^{13} s^{-1}. Our result on Pt(1 1 1) is consistent with previous studies of CH_3–I bond cleavage on Pt(1 1 1) that determined an E_d value of 12.8 kcal/mol [31].

Partial decomposition of chemisorbed CH_3I also causes desorption of CH_4 and H_2 during TPD and leaves carbon on the surface. Fig. 2 compares the H_2 TPD traces for increasing CH_3I exposures on Pt(1 1 1) and the (2×2) alloy. No desorption of H_2 occurred from the $\sqrt{3}$ alloy. On Pt(1 1 1), two main peaks occur, one at 333 K that shifts to 312 K at saturation, and another at 537 K that does not shift with increasing CH_3I exposures. This is consistent with previous reports in the literature [1,5]. The lower temperature peak, which is relatively large at low coverages, is likely to correspond to second-order kinetics due to H_2 desorption that is rate-limited by recombination of surface hydrogen adatoms. On the (2×2) alloy, two H_2 TPD peaks occur at 386 and 543 K, and these do not increase much in size nor shift as the initial CH_3I coverage changes. It is worth mentioning that gas-phase H_2 does not dissociatively chemisorb on the (2×2) alloy [32], and so there is no probability that the H_2 desorption observed from the alloy can originate from coadsorption of H_2 from the background gas.

Methane, CH_4, TPD traces following methyl iodide exposures on Pt(1 1 1) and the (2×2) alloy at 100 K are presented in Fig. 3. No corresponding desorption of CH_4 was observed from the $\sqrt{3}$ alloy. On Pt(1 1 1), a CH_4 desorption peak at 274 K was seen at low coverages. This peak becomes broader and shifts to 294 K with a shoulder at 267 K at high initial CH_3I coverages. Zaera and Hoffmann [5] proposed that methane formation occurred by two different reaction paths that gave rise to two, reaction-rate limited CH_4 TPD peaks. Surface methyl groups formed by CH_3I decomposition are hydrogenated to methane by surface hydrogen which is available from background H_2 adsorption at low CH_3I coverages. However, surface hydrogen is mostly produced from partial dehydrogenation of methyl groups to form methylene at higher methyl iodide coverages, and this production of surface hydrogen controls the CH_4 formation and desorption kinetics.

CH_4 desorption from the (2×2) alloy occurred in a peak fixed at 315 K for any coverage. The other peak at 220 K, which shifts to 186 K as the CH_3I exposure increases, is due to a cracking fraction from CH_3I molecular desorption. The

amount of CH_4 desorbed from the (2×2) alloy is much smaller (5% at saturation) than that from Pt(1 1 1), and the single 315-K peak is an indication that only one reaction path is important on this alloy under UHV conditions. This is consistent with observations that gas-phase H_2 dissociative chemisorption does not occur on this alloy surface [32], and thus H_2 adsorption from the background is eliminated. The 21-K shift to higher temperature in the CH_4 TPD peak upon alloying shows that activation energy for dehydrogenation of CH_3 to CH_2 groups increases on the (2×2) alloy, in an amount estimated to be about 2.2 kcal/mol over that on Pt(1 1 1).

The TPD data in Figs. 1–3 can be quantified to give "uptake plots" that reveal the CH_3I adsorption kinetics, as shown in Figs. 4 and 5. These plots also reveal the partitioning of adsorbed CH_3I into decomposition products (determined as TPD peak areas) for increasing amounts of methyl iodide adsorption on Pt(1 1 1) and both Sn/Pt(1 1 1) alloy surfaces. The saturation coverage for one monolayer of chemisorbed CH_3I on clean Pt(1 1 1) at 100 K in Fig. 4 was set to $\theta^{\text{mono}}_{CH_3I} = 0.20$ ML, based on the results of Zaera and Hoffmann [5],

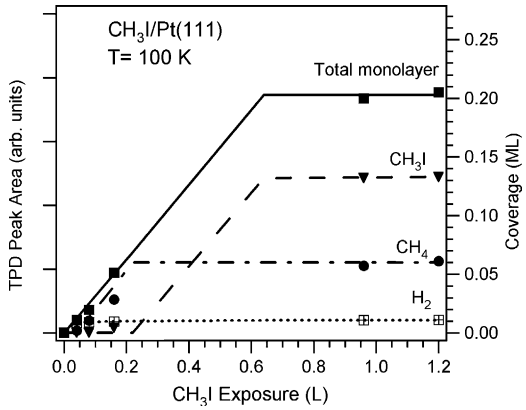

Fig. 4. Uptake curves obtained from TPD results for CH_3I adsorption kinetics at 100 K on Pt(1 1 1) surface. The solid lines are used as a guide to the eye, and incorporate additional information on the emergence of the multilayer CH_3I desorption peak at intermediate exposures.

obtaining $\theta^{\text{rev}}_{CH_3I} = 0.132$ ML in our case. The H_2 TPD peak area due to CH_3I decomposition was calibrated from ethylene decomposition after ethylene exposures on Pt(1 1 1) at 100 K and considering $\theta_{C_2H_4} = 0.25$ ML and $\theta^{\text{dec}}_{C_2H_4} = 0.11$ ML, as reported in previous work [22,26]. According to

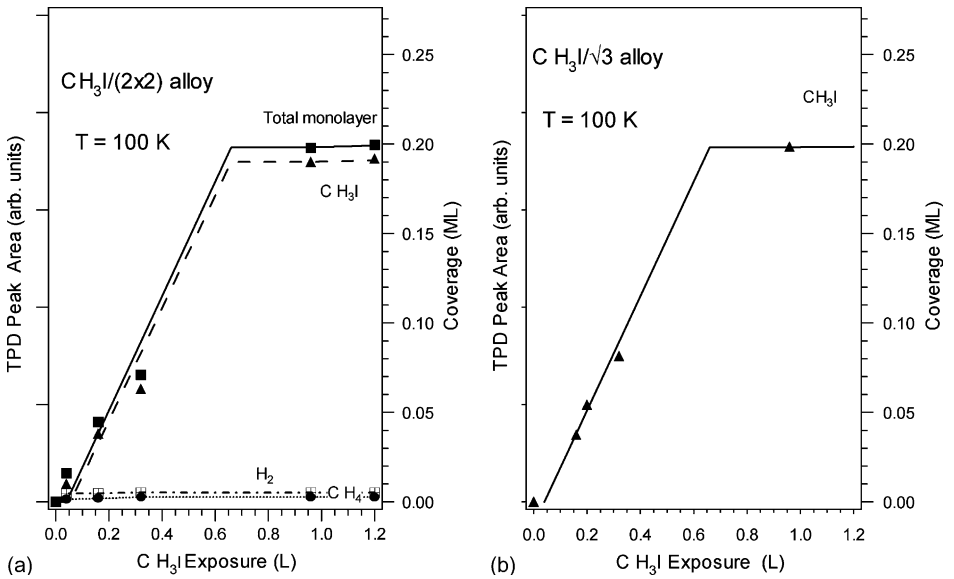

Fig. 5. Uptake curves obtained from TPD results for CH_3I adsorption kinetics at 100 K on (a) the (2×2) and (b) $\sqrt{3}$ Sn/Pt(1 1 1) surfaces at 100 K. Relative CH_3I coverages were obtained by using the integrated CH_3I and H_2 TPD peak areas from Figs. 1–3, with $\theta_{CH_3I} = 0.2$ at 100 K at saturation on Pt(1 1 1) [5]. The solid lines are used as a guide for the eyes.

this estimate, and consistent with a constant value of the CH_3I sticking coefficient during formation of the monolayer, 33.5% of the CH_3I monolayer decomposes into CH_4 and H_2 during TPD, eventually leaving only carbon on the Pt(1 1 1) surface. This amount is lower than the 50% value found by Zaera and Hoffmann [5], and the 63% value of French and Harrison [9]. Possible explanations are that our crystal had fewer defects, or more likely, that we had better control of electron exposure from the ionizer region of the mass spectrometer in the current experiment than in previous work.

A comparison of the CH_3I TPD peak areas establishes that the coverage of chemisorbed CH_3I in the monolayer is the same on all three surfaces. On the (2×2) alloy, the amount of H_2 desorption was about 50% smaller than on Pt(1 1 1). Fig. 5 shows that the monolayer coverage of CH_3I on the (2×2) alloy at 100 K is $\theta^{\text{mono}}_{CH_3I} = 0.20$ ML, with $\theta^{\text{rev}}_{CH_3I} = 0.19$ ML and $\theta^{\text{dec}}_{CH_3I} = 0.01$ ML, i.e., 4% of the monolayer decomposes during TPD. On the $\sqrt{3}$ alloy, completely reversible adsorption of CH_3I occurs without any decomposition. These values are supported by the similar exposures required to form the monolayers on the three surfaces, which would be expected given a constant value of the CH_3I sticking coefficient on all three surfaces at 100 K.

Fig. 6 shows the vibrational spectrum of a CH_3I multilayer on the (2×2) alloy at 100 K. Energy loss peaks at 515, 895, 1254, 1435, 2970 and 3065 cm^{-1} can be assigned to molecular CH_3I modes as ν(C–I), $\rho(CH_3)$, $\delta_s(CH_3)$, $\delta_a(CH_3)$, $\nu_s(CH_3)$ and

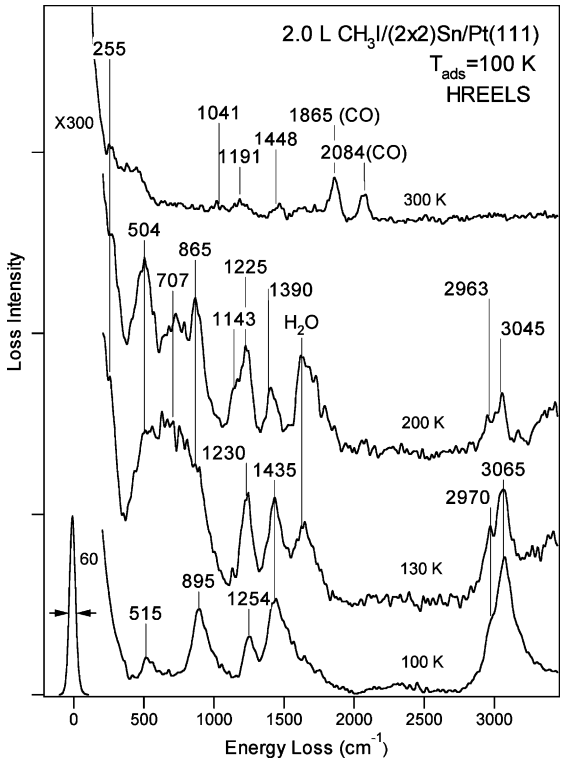

Fig. 6. HREELS spectra obtained after stepwise annealing a saturation dose of methyl iodide on the (2×2) alloy at 100 K.

$\nu_a(CH_3)$, respectively. Table 1 compares the energy loss peaks for the CH_3I multilayer spectrum in Fig. 6 to the vibrations in gaseous CH_3I [33] and previous studies of CH_3I adsorbed on Cu(1 1 1) [8] and Pt(1 1 1) by HREELS [1], and Pt(1 1 1) by IRAS [9]. Vibrational frequencies for CH_3I in the

Table 1
Vibrational frequencies of CH_3I

Normal mode	$CH_3I_{(g)}$ IR [33]	Cu(1 1 1)		Pt(1 1 1)			(2×2) Sn/Pt(1 1 1)	
		HREELS [8] Multilayer $T = 110$ K	HREELS [8] Multilayer $T = 120$ K	IRAS [5,9] Multilayer $T = 100$ K	IRAS [5,9] Monolayer $T = 150$ K	HREELS [1] Monolayer $T = 150$ K	HREELS [This work] Multilayer $T = 100$ K	HREELS [This work] Monolayer $T = 130$ K
$\nu_a(CH_3)$	3060	3050	3045				3065	3065
$\nu_s(CH_3)$	2969	2960	2970	2920, 2905	–, 2905	3025	2970	2970
$\delta_a(CH_3)$	1438	1440	1405	–, 1406	–, 1406	1395	1435	1435
$\delta_s(CH_3)$	1251	1245	1230	1206, 1219	1215, 1215	1220	1254	1230
$\rho(CH_3)$	883	880	875	886, –		875	895	
ν(C–I)	533	535				480	515	
ν(M–I)								255

multilayer on the (2×2) alloy are not perturbed much from values determined by IR spectroscopy for $CH_3I_{(g)}$, as would be expected for a condensed, physisorbed film.

Heating the CH_3I multilayer on the (2×2) alloy from 100 to 130 K removes all physisorbed and multilayer species, but leaves most of the CH_3I adsorbed in the monolayer. Only small shifts occurred in the monolayer spectrum, but the relative intensities of the ν(C–I), $\delta_s(CH_3)$, and $\nu_s(CH_3)$ peaks were increased. This indicates that the CH_3I molecule is still intact, but that the orientation of the C–I bond is more aligned with the surface normal compared to that in the multilayer film. However, the significant intensity of the $\delta_a(CH_3)$ and $\nu_a(CH_3)$ modes establishes that the C–I bond is not perpendicular to the surface. A small shoulder at 255 cm^{-1} is also now detected and associated with the ν(Pt–I) mode. We note that most of the broad loss feature from 500 to 900 cm^{-1} centered at 707 cm^{-1}, and the loss peak near 1625 cm^{-1} is due to co-adsorbed H_2O that accumulated at the surface during acquisition of the HREELS spectrum [8,34].

Henderson et al. [1] proposed that bonding of methyl iodide on Pt (1 1 1) occurs via the iodine atom. Later studies established that chemisorbed methyl iodide on Pt(1 1 1) adopts a tilted configuration (iodine atom down) at low coverages and an upright geometry with C_{3V} symmetry at monolayer coverages [5]. Our results show that methyl iodide adsorbs on the (2×2) alloy near monolayer coverage quite similarly in a relatively upright configuration with the iodine atom next to the surface, but with the C–I bond tilted away from the surface normal. In addition, the vibrational frequencies of methyl iodide adsorbed in the monolayer on the (2×2) alloy are much closer to the physisorbed values than on Pt(1 1 1), which is consistent with a lower adsorption energy on the alloy.

Heating the adlayer on the (2×2) alloy to 200 K desorbs most of the CH_3I from the monolayer, but does not cause any H_2 or CH_4 desorption. This causes the vibrational spectrum to change, with peaks at 504, 865, 1143, 1390, 2963 and 3045 cm^{-1}. Some adsorbed CH_3I remains to contribute the peak at 1225 cm^{-1} and we note again the unfortunate appearance of some features due to coadsorbed water in the spectrum. Based on the CH_4 evolution that eventually occurs in TPD from the alloy, and prior studies of CH_3I on Pt(1 1 1), we sought to establish evidence for the appearance of adsorbed methyl groups in our spectra. We must consider, however, that the concentration is expected to be only one percent of a monolayer or less. The vibrational mode assignments for some representative studies identifying adsorbed CH_3 groups are shown in Table 2. Comparisons to our spectrum obtained after heating to 200 K reveal a credible assignment of chemisorbed methyl groups on the (2×2) alloy with the observed new peaks corresponding to ν(Pt–C), $\rho(CH_3)$, $\delta_s(CH_3)$, $\delta_a(CH_3)$, $\nu_s(CH_3)$ and $\nu_a(CH_3)$ modes, respectively. The appearance of loss peaks from $\delta_s(CH_3)$ and $\delta_a(CH_3)$, along with $\nu_s(CH_3)$ and $\delta_a(CH_3)$, modes with similar intensities indicates that the methyl groups are chemisorbed with their C_{3V} symmetry axis tilted away from the surface normal. This is

Table 2
Vibrational frequencies of CH_3 ligands

Normal mode	$Bi(CH_3)_{3(g)}$ [35]	$Bi(CH_3)_3$/Pt(1 1 1)	Cu(1 1 1)	Pt(1 1 1)			(2×2) Sn/Pt(1 1 1)
		HREELS [35] $T = 150$ K	HREELS [8] $T = 180$ K	HREELS[18] $T = 200$ K	IRAS [5,9] $T = 220$ K	HREELS [1] $T = 260$ K	HREELS [This work] $T = 200$ K
$\nu_a(CH_3)$	3054		2920	2905	–, 2920	2925	3045
$\nu_s(CH_3)$	2994	2971	2830	2852	–, 2880	2775	2963
$\delta_a(CH_3)$	1383	1388	1370	1456	–, 1410	1425	1390
$\delta_s(CH_3)$	1160	1140	1190	1366	1220, 1224	1165	1143
$\rho(CH_3)$	780	789	830	897			865
ν(M–C)	460 (ν(Bi–C))	453 (ν(Bi–C))	345			520	504
ν(M–I)			230				255

similar to the geometry of methyl groups bound on Pt(1 1 1) [9,18].

As shown in Table 2, very close agreement exists between the vibrational frequencies of methyl groups chemisorbed on the (2×2) alloy and bound in molecular $Bi(CH_3)_3$ adsorbed on Pt(1 1 1) [35]. This agreement is better than the comparison to methyl groups bound on Pt(1 1 1). This is reasonable if, as expected, the methyl group is more weakly chemisorbed on the alloy than on Pt(1 1 1), and thus more closely resembles the chemical bonding between CH_3 and Bi, a main group metal much less reactive than Pt.

As shown in the top curve following heating to 300 K, the trace amount of chemisorbed hydrocarbon fragments cause small loss peaks at 1041, 1191 and 1448 cm^{-1} which correspond to δ(CH) modes for these species, possibly a mixture of fragments such as CH in different configurations [36]. The peak at 255 cm^{-1} is due to the ν(Pt–I) mode, and coadsorbed CO causes the loss peaks at 1865 and 2084 cm^{-1} [32]. The species that remain adsorbed on the alloy at 300 K are due to dehydrogenation and or condensation of methyl groups. Methylene (CH_2) groups, observed by Zaera on Pt (1 1 1) under similar conditions [19], are likely intermediates in this chemistry, but CH_2(a) vibrations are not consistent with the spectrum obtained from the alloy at 300 K.

Fig. 7 summarizes the influence of alloying Sn into the Pt(1 1 1) surface with regard to several parameters describing the adsorption, desorption and reaction of CH_3I. Fig. 7 compares the amount of CH_3I decomposition on Pt(1 1 1) and two alloys. Alloying the Pt(1 1 1) surface with Sn strongly suppresses CH_3I decomposition, by an order of magnitude on the (2×2) alloy with $\theta_{Sn} = 0.25$ and completely on the $\sqrt{3}$ alloy with $\theta_{Sn} = 0.33$. We have previously pointed out that the absence of adjacent threefold "pure Pt" sites on the (2×2) alloy and the absence of any threefold "pure Pt" sites on the $\sqrt{3}$ alloy might play an important role in the low reactivity of these alloys. Such sites or "ensembles" would be expected to stabilize the transition state and the $I_{(a)}$ reaction product from CH_3I decomposition. Alloying affects the CH_3I adsorption energy to a smaller extent. These energies are equivalent to the thermal desorption

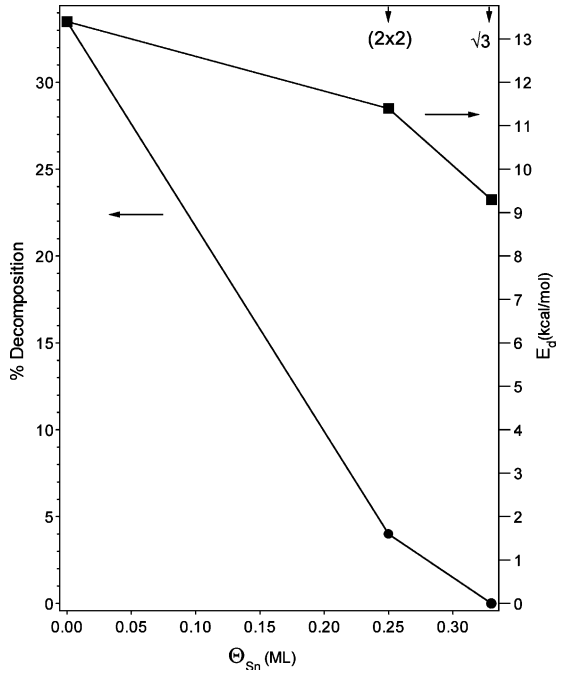

Fig. 7. Comparison of fraction of CH_3I decomposition on Pt(1 1 1) and Sn/Pt(1 1 1) alloy surfaces. Corresponding desorption activation energies for CH_3I adsorption on these surfaces are also shown and scaled on the right hand side.

activation energies E_d for CH_3I on these surfaces. Values of E_d, as estimated by Redhead analysis [29], are given on the right hand side of Fig. 7. Removal of the threefold "pure Pt" sites on the $\sqrt{3}$ alloy appears to cause a much larger effect on the CH_3I adsorption energy than would be expected simply based on the amount of Sn in the surface layer such as might be estimated based on the data from the (2×2) alloy. It is instructive to also compare all of these values to our estimated value of 8 kcal/mol for the sublimation energy of CH_3I from the condensed multilayer.

The following elementary reaction steps can account for the H_2 and CH_4 products observed in TPD from the reaction of CH_3I on the (2×2) Sn/Pt(1 1 1) alloy:

$$CH_3I \rightarrow CH_{3(a)} + I_{(a)}, \quad 130 < T < 200\ \text{K} \qquad (1)$$

$$CH_{3(a)} \rightarrow CH_{2(a)} + H_{(a)}, \quad 200 < T < 300\ \text{K} \qquad (2)$$

$$CH_{3(a)} + H_{(a)} \rightarrow CH_{4(g)}, \quad T > 270\ \text{K} \quad (T_p = 315\ \text{K}) \tag{3}$$

$$CH_{2(a)} \rightarrow CH_{(a)} + H_{(a)}, \quad 200 < T < 300\ \text{K} \tag{4}$$

$$2H_{(a)} \rightarrow H_{2(g)}, \quad T > 340\ \text{K} \quad (T_p = 386\ \text{K}) \tag{5}$$

$$nCH_{(a)} \rightarrow C_{n(a)} + nH_{(a)}, \quad T > 500\ \text{K} \quad (T_p = 543\text{K}) \tag{6}$$

The absence of C_2H_4 and C_2H_6 desorption, even though these molecules are reversibly adsorbed on the alloy, indicates that C–C bond coupling reactions such as the recombination of CH_3 groups are negligible under these conditions.

Low energy electron induced dissociation (EID) of multilayers of cyclohexane [23] and C_5–C_8 cycloalkanes [25] has been used previously to prepare cycloalkyl intermediates on Pt(1 1 1) and Sn/Pt(1 1 1) surface alloys. Generally, cycloalkenes and H_2 are the main species desorbed after EID of multilayer cycloalkanes on Pt(1 1 1) and Sn/Pt(1 1 1) alloy surfaces. In addition, benzene desorption also occurred after EID of multilayer C_6–C_8-cycloalkane films on both Pt–Sn surface alloys. Thus, cycloalkyl dehydrogenation occurs extensively on both Sn/Pt(1 1 1) alloys, and hence, it is evident that CH_3I cannot be used reliably as a thermal precursor under UHV conditions to yield $CH_{3(a)}$ on Pt–Sn alloys. A solution to preparing high coverages of chemisorbed CH_3 species on these alloys for study is to use a pyrolytic source of CH_3 radicals [17,18] and we have such studies currently underway in our laboratory. Other non-thermal methods, such as EID or photochemical activation of CH_3I could also be considered.

4. Conclusions

Two ordered Sn/Pt(1 1 1) surface alloys with $\theta_{Sn} = 0.25$ and 0.33 ML exhibit a lower adsorption energy and reactivity of methyl iodide (CH_3I) than the Pt(1 1 1) surface. Molecular binding energies are reduced to 11.4 kcal/mol on the (2×2) alloy and 9.3 kcal/mol on the $\sqrt{3}$ alloy from 13.4 kcal/mol on Pt(1 1 1). On Pt(1 1 1) at 100 K, one-third of the chemisorbed layer decomposes to form CH_4 and H_2 during TPD, leaving carbon on the surface. Alloying with Sn caused a large increase in the amount of reversibly adsorbed CH_3I. The presence of 25% Sn atoms in the (2×2) alloy surface layer suppressed the CH_3I decomposition to 4%. Only CH_4 and H_2 were detected during TPD and adsorbed methyl (CH_3) groups were identified at 200 K. Completely reversible adsorption and desorption of CH_3I occurred on the $\sqrt{3}$ alloy with $\theta_{Sn} = 0.33$ and no decomposition was observed. The absence of adjacent threefold "pure Pt" sites on the (2×2) alloy and the absence of any threefold "pure Pt" sites on the $\sqrt{3}$ alloy which may be required to stabilize the transition state or $I_{(a)}$ reaction product is consistent with these results and this might play an important role in the low reactivity of these alloys. This eliminates the use of CH_3I, and presumably other alkyl halides, as a thermal precursors under UHV conditions to yield $CH_{3(a)}$ and other hydrocarbon intermediates on Pt–Sn alloys.

Acknowledgements

This work was supported by the US Department of Energy, Office of Basic Energy Sciences, Chemical Sciences Division. Dr. E.C. Samano thanks financial support through CONACYT and DGAPA-UNAM. We thank Dr. Hong He for his assistance in the HREELS experiments.

References

[1] M.A. Henderson, G.E. Mitchell, J.M. White, Surf. Sci. 184 (1987) L325.
[2] F. Zaera, Surf. Sci. 219 (1989) 453.
[3] F. Zaera, J. Phys. Chem. 94 (1990) 8350.
[4] F. Zaera, H. Hoffmann, P.R. Griffiths, J. Electron Spec. Relat. Phenom. 54/55 (1990) 705.
[5] F. Zaera, H. Hoffmann, J. Phys. Chem. 95 (1991) 6297.
[6] M.A. Henderson, G.E. Mitchell, J.M. White, Surf. Sci. 248 (1991) 279.
[7] H. Hoffman, P.R. Griffiths, F. Zaera, Surf. Sci. 262 (1992) 141.
[8] J.-L. Lin, B.E. Bent, J. Vac. Sci. Technol. A 10 (1992) 2202.
[9] C. French, I. Harrison, Surf. Sci. 342 (1995) 85.
[10] A. Kis, K.C. Smith, J. Kiss, F. Solymosi, Surf. Sci. 460 (2000) 190.
[11] J. Kiss, R. Barthos, F. Solymosi, Top. Catal. 14 (2001) 145.

[12] J.J. Rooney, J. Mol. Catal. 31 (1985) 147.
[13] M.P. Kaminsky, N. Winograd, G.L. Geoffroy, M.A. Vannice, J. Am. Chem. Soc. 108 (1986) 1315.
[14] M.B. Lee, Q.Y. Yang, S.L. Tang, S.T. Ceyer, J. Chem. Phys. 85 (1986) 1693.
[15] D. Strongin, J. Mowlem, Chem. Phys. Lett. 187 (1991) 281.
[16] C.-M. Chiang, B.E. Bent, Surf. Sci. 279 (1992) 79.
[17] X.-D. Peng, R. Viswanathan, G.H. Smudde Jr., P.C. Stair, Rev. Sci. Instrum. 63 (1992) 3930.
[18] D. Jentz, M. Trenary, X.D. Peng, P.C. Stair, J. Fan, Surf. Sci. 341 (1995) 282.
[19] F. Zaera, Langmuir 7 (1991) 1998.
[20] M.T. Paffett, S.C. Gebhard, R.G. Windham, B.E. Koel, Surf. Sci. 223 (1989) 449.
[21] C. Xu, B.E. Koel, M.T. Paffett, Langmuir 10 (1994) 166.
[22] Y.-L. Tsai, C. Xu, B.E. Koel, Surf. Sci. 385 (1997) 37.
[23] C. Xu, B.E. Koel, Surf. Sci. 292 (1993) L803.
[24] C. Xu, Y.-L. Tsai, B.E. Koel, J. Phys. Chem. 98 (1994) 585.
[25] Y.-L. Tsai, B.E. Koel, Langmuir 14 (1998) 1290.
[26] R.G. Windham, M.E. Bartram, B.E. Koel, J. Phys. Chem. 92 (1988) 2862.
[27] M.T. Paffett, R.G. Windham, Surf. Sci. 208 (1989) 34.
[28] S.H. Overbury, D.R. Mullins, M.T. Paffett, B.E. Koel, Surf. Sci. 254 (1991) 45.
[29] P.A. Redhead, Vacuum 12 (1962) 203.
[30] C.T. Campbell, Y.K. Sun, W.H. Weinberg, Chem. Phys. Lett. 179 (1991) 53.
[31] M.B. Huggenschmidt, M.E. Domagala, C.T. Campbell, Surf. Sci. 275 (1992) 121.
[32] M.T. Paffett, S.C. Gebhard, R.G. Windham, B.E. Koel, J. Phys. Chem. 94 (1990) 6831.
[33] L.M. Sverdlov, M.A. Kovner, E.P. Krainov, Vibrational Spectra of Polyatomic Molecules, Wiley, Jerusalem, 1974.
[34] B. Rowland, M. Fisher, J.P. Devlin, J. Phys. Chem. 97 (1993) 2485.
[35] M.E. Pansoy-Hjelvik, R. Xu, Q. Gao, K. Weller, F. Feher, J.C. Hemminger, Surf. Sci. 312 (1994) 97.
[36] Q.Y. Yang, K.J. Maynard, A.D. Johnson, S.T. Ceyer, J. Phys. Chem. 102 (1995) 7734.